One-Electron Oxidation of Selenourea in Aqueous Solution

B. Mishra, D. K. Maity,* K. I. Priyadarsini, H. Mohan,* and J. P. Mittal

Radiation Chemistry and Chemical Dynamics Division, Bhabha Atomic Research Centre, Trombay, Mumbai 400 085, India

Received: October 14, 2003; In Final Form: December 19, 2003

One-electron oxidation of selenourea in aqueous solution has been studied using pulse radiolysis, cyclic voltammetry, and ab initio quantum chemical techniques. Specific one-electron oxidants ($N_3^{\bullet}$, $Br_2^{\bullet-}$, $Cl_2^{\bullet-}$, $I_2^{\bullet-}$) react with selenourea to form a broad transient optical absorption band with the maximum absorption at the wavelength (λ_{max}) of 410 nm. The hydroxyl radical reacts with selenourea at a bimolecular rate constant of $k = 9.9 \times 10^9$ M^{-1} s^{-1} and a similar transient band at $\lambda_{max} = 410$ nm is formed. The absorbance at 410 nm has been observed to be dependent on solute concentration. The transient band at 410 nm is assigned to the selenourea dimer radical cation. The transient shows reactivity toward oxygen ($k = 8.6 \times 10^7$ M^{-1} s^{-1}). The $H^{\bullet}$ atom is observed to react with selenourea with a bimolecular rate constant of 2.1×10^9 M^{-1} s^{-1}, giving a transient optical absorption band at 410 nm, which is also assigned to the same dimer radical cation formed following the H-abstraction reaction. Redox reaction studies in aqueous solution by pulse radiolysis and cyclic voltammetry revealed that the one-electron oxidation potential of selenourea is less than that of its lighter analogues, thiourea and urea. The theoretical result that is based on the ab initio quantum chemical method confirms that the transient optical absorption band at 410 nm is due to the dimer radical cation of selenourea. The calculation, which is based on nonlocal correlated hybrid density functional theory, illustrates the formation of an *intermolecular two-center, three-electron* (2c−3e) bond between two Se atoms with a binding energy of 21.1 kcal/mol.

1. Introduction

The radiation-induced chemistry of organic sulfur and selenium compounds in aqueous solution is very important, because the radicals and ions generated from these compounds have an important role in understanding many chemical and biological processes. Such studies are of current interest, because these radical species are considered to be possible intermediates in redox reactions of sulfur-/selenium-containing biomolecules and finding application as radioprotectors.[1−9] Recently, the interest in the chemistry of selenium-containing compounds has increased, because of the applications in synthesis and organic conductors. Organoselenium compounds such as isoselenocyanates, selenoformamide, and selenoureas are important building blocks for the synthesis of biologically important selenium compounds. Many cyclic selenoureas have also found application in carbohydrate chemistry research.[10]

Hydroxyl radicals and many one-electron oxidants are known to react with dialkyl sulfides (R_2S) in aqueous solution to form a sulfur-centered dimer radical cation $(R_2S)_2^{\bullet+}$ via a complex sequence of reactions that involve the OH adduct, the α-thio radical, and the monomer radical cation. The monomer system with the singly oxidized S atom is normally unstable and has a high tendency to stabilize when it is coordinated to another S atom or other heteroatoms, such as P, O, N, and halogen atoms through *intermolecular* or *intramolecular* interaction.[11−16] This interaction results in the formation of a new *three-electron* σ-bond that contains two bonding σ electrons and one antibonding σ* electron (>S∴S<). The presence of an aryl group results in the formation of a stable monomer radical cation, because of the resonance stabilization of the free electron in the benzene π-ring.[17−20] On the other hand, in the case of thiourea and its derivatives, the semioxidized species has been assigned to the delocalization of the free electron over the −N−C−S− system.[21] Wang et al.[22] studied the OH-radical-induced oxidation of thiourea and tetramethylthiourea and showed the formation of a sulfur-centered dimer radical cation in the reversible equilibrium with a monomer radical cation.

Although some of the properties of organic selenium compounds are similar to their sulfur counterparts (group 16 of the periodic table), selenol (−SeH) is known to be a more powerful nucleophile than thiol (−SH). In general, the chemistry of selenium and tellurium compounds has been observed to be different from their lighter analogues. This is mainly due to the difference in the electronegativity, polarizablitity, and availability of d-orbitals for bonding.[23,24] The −SeH group of selenocysteine in proteins has a pK_a value of ∼5.2 and is present in the dissociated form at physiological pH, whereas −SH is present in the protonated form, because of its higher pK_a value of 8.6.[5,8] It has been shown for several enzymes that the incorporation of a more chemically reactive −SeH group into the active center, instead of −SH, results in better catalytic action. The organoselenium compounds are also important, because they are known to catalyze the reduction of hydroperoxides and protect the cell membrane from oxidative damage. It has also been reported that some enzyme-catalyzed redox reactions require the participation of selenium-containing proteins. The radiation-induced chemistry of organic sulfur compounds has been reasonably well understood, and a large number of reports are available in the literature.[11−16] On the other hand, only a few reports have appeared in the literature on the

* Authors to whom correspondence should be addressed. E-mail addresses: dkmaity@magnum.barc.ernet.in, harim@apsara.barc.ernet.in.

10.1021/jp0371130 CCC: $27.50
Published on Web 02/05/2004

radiation-induced free-radical chemistry of organoselenium compounds.[17,25]

Therefore, it is important to study the nature and the redox properties of the transient species generated from organoselenium compounds under different environments. With this objective, a detailed free-radical chemistry of organoselenium compounds has been initiated, and the results of the one-electron oxidation of selenourea have been reported here. To assign the definite structure and nature of bonding of the intermediate transient species, we have also used ab initio quantum chemical methods. The structure, bonding, and various molecular properties of selenourea, its radical cation, and the dimer radical cation have been studied and compared the same features of thiourea and urea systems. We are able to provide definite evidence of the formation of an *intermolecular three-electron* σ-bond between two Se atoms (>Se∴Se<) in the dimer radical cation of selenourea, making the transient species stable and detectable on the microsecond time scale.

2. Experimental Section

Materials. Selenourea was obtained from Aldrich Chemicals and used without any further purification. All other chemicals and reagents were of "Analar" grade and used as such. Solutions were prepared in "nanopure" water that had a conductivity of 0.1 μS cm^{-1} (obtained from a Barnstead Nanopure water system), and freshly prepared solutions were used for each experiment. The ground-state absorption spectra were recorded on a Hitachi model 330 spectrometer. The pH values of the solutions were adjusted using $HClO_4$, $Na_2HPO_4{\cdot}2H_2O$, KH_2PO_4, and NaOH. All other experimental details are described elsewhere.[26] Cyclic voltammetry studies were performed on Ecochemie Auto Lab (PGSTAT 20 Model) and through the use of a conventional three-electrode system (i.e., glassy carbon working electrode, platinum wire as the auxiliary electrode, and an Ag−AgCl reference electrode).

Pulse Radiolysis Studies. The pulse radiolysis experiments were performed with high-energy electron pulses (7 MeV, 50 ns) obtained from a linear electron accelerator; the details are given elsewhere.[27] An aerated aqueous solution of KSCN (1×10^{-2} M) was used to determine the dose delivered per pulse, using $G\epsilon_{500} = 21520$ M^{-1} cm^{-1} per 100 eV for the transient $(SCN)_2^{\bullet-}$ species.[28] G denotes the number of species per 100 eV of absorbed energy ($G = 1$ corresponds to 0.1036 μmol J^{-1}), and ϵ is the molar absorptivity of the $(SCN)_2^{\bullet-}$ species at 500 nm. The dose per pulse was ~8 Gy (1 Gy = 1 J kg^{-1}).

The transient species formed on pulse radiolysis were detected via the optical absorption method, using a 450 W pulsed xenon arc lamp and a Kratos model GM-252 monochromator. The photomultiplier output was digitized with a 100 MHz storage oscilloscope that was interfaced to a computer for kinetic analysis.[29] The bimolecular rate constants (k) were determined from the linear regression plots of k_{obs} versus solute concentration for at least three independent experiments, and the variation was within 10%. The pulse radiolysis experiments were performed in suprasil cuvettes with a cross-sectional area of 1 cm^2 at 25 °C.

Radiolysis of a N_2-saturated neutral aqueous solution leads to the formation of three highly reactive species ($^{\bullet}H$, $^{\bullet}OH$, e_{aq}^-), in addition to the less-reactive or inert molecular products (H_2, H_2O_2, and H_3O^+).[30]

$$H_2O \rightarrow {}^{\bullet}H,\ {}^{\bullet}OH,\ e_{aq}^-,\ H_2,\ H_2O_2,\ H_3O^+ \qquad (1)$$

The reaction with $^{\bullet}OH$ radicals was performed in N_2O-saturated solutions, where e_{aq}^- is quantitatively converted to $^{\bullet}OH$ radicals and the $^{\bullet}OH$ radical is the main species to react with the solute.

$$N_2O + e_{aq}^- \rightarrow {}^{\bullet}OH + OH^- + N_2 \qquad (2)$$

The reactions of specific one-electron oxidants were conducted under conditions such that the $^{\bullet}OH$ radicals do not react with the solute and only the one-electron oxidants react with the solute. Specific one-electron oxidants ($Br_2^{\bullet-}$, $I_2^{\bullet-}$, and $Cl_2^{\bullet-}$) were generated by the pulse radiolysis of 5×10^{-2} M aqueous solutions of KBr, KI, and KCl, respectively, according to the following equations:[31]

$$X^- + {}^{\bullet}OH \rightarrow X^{\bullet} + OH^- \qquad (3a)$$

$$X^{\bullet} + X^- \leftrightarrows X_2^{\bullet-} \qquad (3b)$$

where X = Br, Cl, and I. $Cl_2^{\bullet-}$ was generated in an aerated solution at pH 1, and $Br_2^{\bullet-}$ and $I_2^{\bullet-}$ were generated in a N_2O-saturated solution at pH 7. The $N_3^{\bullet}$ radical was produced when a N_2O-saturated solution that contained 0.1 M NaN_3 was subjected to pulse radiolysis, according to the following equation:

$$N_3^- + {}^{\bullet}OH \rightarrow N_3^{\bullet} + OH^- \qquad (4)$$

The reaction of the $^{\bullet}H$ atom was studied at pH 1 in a N_2-saturated solution that contained *tert*-butyl alcohol (0.3 M) to scavenge $^{\bullet}OH$ radicals (reaction 5):

$$(CH_3)_3COH + {}^{\bullet}OH \rightarrow {}^{\bullet}CH_2(CH_3)_2COH + H_2O \qquad (5)$$

Theoretical Studies. Previous reports showed that Becke's half-and-half (BHH) nonlocal exchange and Lee−Yang−Parr (LYP) nonlocal correlation functionals (BHHLYP) performed well to describe three-electron, bonded, open-shell doublet systems.[32] The BHHLYP functional included 50% Hartree−Fock exchange, 50% Slater exchange, and the additional correlation effects of the LYP functional. Various searches were performed without any symmetry restriction to predict the geometry of the most-stable conformer of selenourea, thiourea, and urea, their radical cations, and the dimer radical cations under gas-phase isolated conditions. The gas-phase molecular geometry was further optimized fully, including solvent effects, by following the Onsager reaction field model with the cavity radius based on the gas-phase optimized geometry. The symmetry-breaking instability problem in optimizing the molecular geometry was also examined.[33] Hessian calculation was also done at the BHHLYP level, to examine the nature of the stationary geometry. Calculation was also performed to determine the excitation wavelength needed to excite an electron from the highest doubly occupied bonding orbital to the lowest singly occupied antibonding orbital ($\sigma \rightarrow \sigma^*$) of the respective dimer radical cation at the CIS (CI singles) level of theory. To include the solvent effect in the CIS calculation, the fully optimized geometry and orbitals, including solvent effects, were used to determine the absorption maxima (λ_{max}) in solution. All these calculations were performed by adopting the GAMESS suite of programs on a PC-based LINUX cluster platform.[34] Visualization of the geometry and relevant molecular orbitals was done by following the MOLEKEL program system.[35]

3. Results and Discussion

Pulse Radiolysis Studies. The ground-state optical absorption spectrum of selenourea (SeU) showed absorption bands at 225

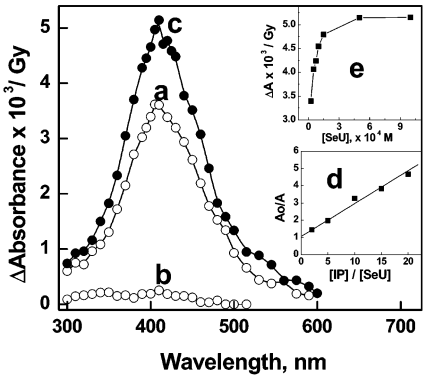

Figure 1. Difference transient optical absorption spectra (normalized) obtained when a N_2O-saturated aqueous solution (pH 7) of selenourea 5×10^{-5} M is subjected to pulse radiolysis in the (a) absence and (b) presence of *tert*-butyl alcohol (0.3 M). Plot c shows the difference transient optical absorption spectra obtained when a N_2O-saturated aqueous solution (pH 7) of 1×10^{-3} M SeU is subjected to pulse radiolysis in the absence of *tert*-butyl alcohol. Panel d shows a competition kinetics plot of the $^{\bullet}$OH radical reaction with SeU and 2-propanol for absorbance at 410 nm, and Panel e shows the variation of absorbance at 410 nm as a function of the SeU concentration.

($\epsilon = 8.7 \times 10^3$ M^{-1} cm^{-1}) and 255 nm ($\epsilon = 9.5 \times 10^3$ M^{-1} cm^{-1}) with increasing absorption at $\lambda < 210$ nm and without any appreciable absorption at $\lambda > 300$ nm. Therefore, pulse radiolysis studies in the wavelength region of 300−700 nm, using the optical absorption detection technique, could be used without any correction for the ground-state absorption. The nature of the spectrum remained the same in the pH range of 1−11 and did not exhibit any change in the spectrum with time, which showed the solution to be stable and also showed the absence of any solute pK_a in this pH region. At pH >11, the solution is stable up to 30 min but showed decomposition after prolonged storage. The pulse radiolysis studies are restricted in the pH range of 1−11.

Figure 1a shows the transient optical absorption spectrum ($\lambda_{max} = 410$ nm) obtained when a N_2O-saturated aqueous solution of SeU (5×10^{-5} M, pH 7) was subjected to pulse radiolysis. In the presence of *tert*-butyl alcohol (0.3 M), which is an efficient $^{\bullet}$OH radical and weak H atom scavenger, small absorption (ΔO.D. = 0.004 at 410 nm) was observed in the 300−600 nm region (see Figure 1b). These results suggest that the contribution of the H$^{\bullet}$ atom reaction with SeU (pH 7) is small and the absorption spectrum (Figure 1a) is mainly due to the reaction of $^{\bullet}$OH radicals with SeU. The rate constant for the reaction of $^{\bullet}$OH radicals with SeU was determined by competition kinetic studies, using 2-propanol (IP) as the standard solute. The two competing reactions that are involved lead to the following relationship:

$$^{\bullet}OH + (CH_3)_2CHOH \rightarrow (CH_3)_2{}^{\bullet}COH + H_2O \quad (6)$$

$$^{\bullet}OH + SeU \rightarrow \text{product} \quad (7)$$

$$\frac{A_0}{A} = 1 + \frac{k_{IP+OH}}{k_{SeU+OH}} \times \frac{[IP]}{[SeU]} \quad (8)$$

A_0 and A are the absorbance at 410 nm in the absence and presence of IP, respectively. The transient absorbance at 410 nm was determined for various concentrations of IP (2.5×10^{-3}−1×10^{-2} M) that contained a constant concentration of SeU (5×10^{-4} M). From the slope of the linear plot in Figure 1d, and using a value of $k_{IP+OH} = 1.9 \times 10^9$ M^{-1} s^{-1}, the bimolecular rate constant is determined to be 9.9×10^9 M^{-1} s^{-1} (Table 1).[36] Under the experimental conditions of Figure 1a, ~95% of the $^{\bullet}$OH radicals should have reacted with SeU to form the transient absorption band at 410 nm; however, the transient absorbance at 410 nm was observed to increase with the solute concentration (see Figure 1e), reaching a saturation value only at a SeU concentration of 1×10^{-3} M (see Figure 1c). This increase in the absorbance could not be due to the direct reaction of $^{\bullet}$OH radicals with a higher concentration of SeU: this increase was due to the reaction of the initial transient species with the solute to form a new transient species, probably a dimer radical species. The absorption spectrum for a 1 mM concentration of SeU is shown as Figure 1c, which has same λ_{max} value but with higher absorbance.

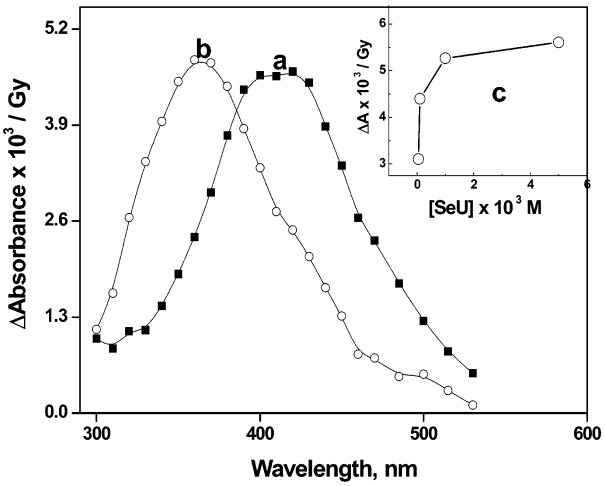

Figure 2. Difference transient optical absorption spectra (normalized) obtained when a N_2O-saturated aqueous solution (pH 7) of Br^- (5×10^{-2} M) containing SeU (3×10^{-4} M) is subjected to pulse radiolysis: (a) 6 μs and (b) 0.5 μs after the pulse, Panel c shows the variation of absorbance (410 nm) as a function of SeU concentration.

TABLE 1: Bimolecular Rate Constant for the Reaction of Different Radical Species with Selenourea (SeU) at pH 7

reaction	bimolecular rate constant, k (M^{-1} s^{-1})
$^{\bullet}OH + SeU$	9.9×10^9
$Br_2^{\bullet-} + SeU$	4.1×10^9
$Cl_2^{\bullet-} + SeU^a$	3.6×10^9
$I_2^{\bullet-} + SeU$	2.8×10^8
$H^{\bullet} + SeU^a$	2.1×10^9

[a] At pH 1.

Hydroxyl radicals are known to react with organic compounds via more than one mechanism (addition, abstraction, electron transfer). The reaction with specific one-electron oxidants was performed to establish the nature of the $^{\bullet}$OH radical reaction with SeU. $Br_2^{\bullet-}$, which is a specific one-electron oxidant, was used to study the one-electron oxidation of SeU. Time-resolved studies on the pulse radiolysis of a N_2O-saturated aqueous solution (pH 7) of Br^- (5×10^{-2} M) that contained 3×10^{-4} M SeU showed the formation of a transient band at 410 nm (Figure 2a) when the $Br_2^{\bullet-}$ absorption band at 350 nm decayed (see Figure 2b). The band at 410 nm should be due to the one-electron oxidized species of SeU. The absorbance at 410 nm was also observed to increase as the SeU concentration increased (see Figure 2c). The Br^- concentration is high enough to scavenge the entire yield of $^{\bullet}$OH radicals. The rate constant for the reaction of $Br_2^{\bullet-}$ with SeU was determined from the decay of $Br_2^{\bullet-}$ at 350 nm, as a function of the SeU concentration (5×10^{-5}−1.75×10^{-4} M). The pseudo-first-order rate constant (k_{obs}) increased linearly as the SeU concentration increased, and

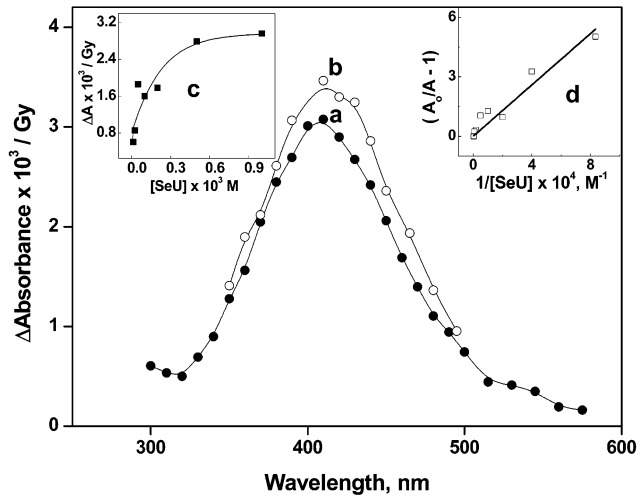

Figure 3. Difference transient optical absorption spectra (normalized) obtained after the pulse radiolysis of an aqueous solution of SeU (250 μM, pH 1, 0.3 M *tert*-butyl alcohol) in (a) N_2 and (b) aerated conditions ([SeU] = 300 μM). Panel c shows the variation of normalized absorbance at 410 nm as a function of [SeU], and panel d shows the linear plot according to eq 9.

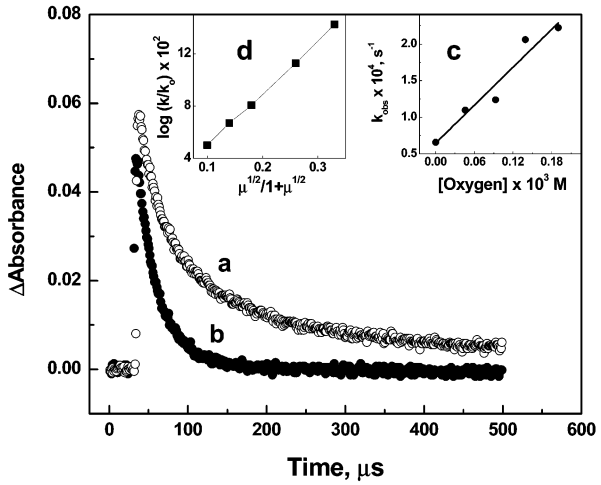

Figure 4. Absorption-time profiles at 410 nm formed after the pulse radiolysis of an aqueous solution of SeU (1×10^{-3} M, pH 7) in (a) N_2O and (b) N_2O-O_2. Panel c shows the variation of the pseudo-first-order rate constant (k_{obs}) as a function of O_2 concentration, and panel d shows the effect of ionic strength on the decay rate of the dimer radical cation at 410 nm.

the bimolecular rate constant is determined to be 4.1×10^9 M^{-1} s^{-1} (see Table 1). The rate constant for the reaction of $Br_2^{\bullet-}$ with SeU was not determined from the formation kinetics at 410 nm, because this band is formed due to a complex process that involves one-electron oxidation and subsequent dimerization.

$Cl_2^{\bullet-}$ and $I_2^{\bullet-}$ were observed to react with SeU with bimolecular rate constants of 3.6×10^9 and 2.8×10^8 M^{-1} s^{-1}, respectively (see Table 1). The rate constant for the reaction of $Cl_2^{\bullet-}$ and $I_2^{\bullet-}$ with SeU was determined from the decay of the transient absorption bands of $Cl_2^{\bullet-}$ and $I_2^{\bullet-}$, respectively, as a function of the SeU concentration. In all these reactions, time-resolved studies showed the formation of a transient optical absorption band at 410 nm and the absorbance increased as the SeU concentration increased.

Pulse radiolysis of a N_2-saturated acidic (pH 1) aqueous solution of SeU (3×10^{-4} M) that contained *tert*-butyl alcohol (0.3 M) showed the formation of a transient absorption band at $\lambda_{max} = 410$ nm (Figure 3a), which has been attributed to the transient that is formed when H$^\bullet$ reacts with SeU. In this case, the absorbance at 410 nm also increases as the SeU concentration increases (see Figure 3c), even after the initial reaction with the H atom is complete. The rate constant for the reaction of $^\bullet$H with SeU was determined by competition kinetics, using methyl viologen (MV^{2+}) as a reference solute. Using a value of $k_{H+MV^{2+}} = 6 \times 10^8$ M^{-1} s^{-1}, the bimolecular rate constant for the reaction of SeU with H was determined to be 2.1×10^9 M^{-1} s^{-1}.[37] A smaller rate constant for the reaction of the H$^\bullet$ atom, as compared to that with the $^\bullet$OH radical (9.9×10^9 M^{-1} s^{-1}), suggests that the reaction of the H$^\bullet$ atom occurs via H-abstraction. The $HO_2^\bullet$ radical has also been observed to react with SeU, with the formation of a transient absorption band at $\lambda_{max} = 410$ nm (see Figure 3b). The equilibrium constant for the dimer radical cation, which is formed during the reaction with the H$^\bullet$ atom (pH 1), was determined to be 2.3×10^4 M^{-1} (see Figure 3d).

The nature of the transient optical absorption spectrum obtained on reaction of $^\bullet$OH radicals with SeU is similar to that obtained on reaction with specific one-electron oxidants. Therefore, the transient optical absorption band with $\lambda_{max} =$ 410 nm could be assigned to the one-electron oxidized species of SeU. A similar transient was observed on reaction of $^\bullet$H and $HO_2^\bullet$ radicals with SeU. In all these cases, the band at 410 nm is assigned to the dimer radical cation (Scheme 1). Time-resolved studies did not indicate the formation of any new absorption bands, which suggests that other transient species such as the OH-adduct, radical species formed by H-abstraction, or the solute monomer radical cation could not be observed under the present experimental setup.

SCHEME 1

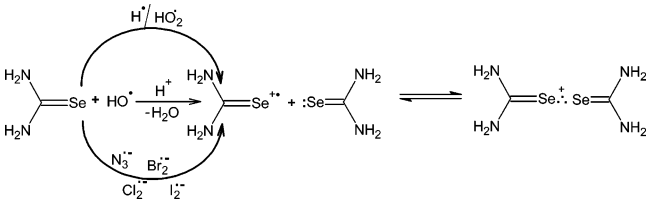

In the absence of oxygen, the band at 410 nm decayed by second-order kinetics, with a $2k$ value of 2.7×10^9 M^{-1} s^{-1} (Figure 4a). Normally, oxygen has no effect on the decay of the dimer radical cation that is formed when dialkyl sulfides are oxidized. However, a few exceptions are reported in the literature; for example, the sulfur-centered dimer radical cation of thiourea reacts with oxygen with a bimolecular rate constant of 1.2×10^7 M^{-1} s^{-1}.[22] In the case of SeU, the decay of the transient band was also observed to be faster in the presence of oxygen (Figure 4b). The pseudo-first-order decay rate constant (k_{obs}) increased linearly as the oxygen concentration increased (see Figure 4c). The slope of the linear plot gave a bimolecular rate constant of 8.6×10^7 M^{-1} s^{-1}. One of the reasons for such unusual reactivity of the dimer radical cation with oxygen could be the fact that one of the possible resonating structures of the dimer radical cation is a carbon-centered radical, which would react with oxygen to form a peroxyl-type radical.[22]

In case of sulfur compounds, the increase in the absorbance was explained by the existence of an equilibrium between the monomer and its dimer radical cation.[11,13] In analogy to sulfur compounds, the increase in the absorbance with SeU concentration is also attributed to the existence of an equilibrium, as shown in Scheme 1. The association constant (K) for this

TABLE 2: Comparison of Different Calculated Properties of Selenourea, Thiourea, and Urea Including the Solvent Effect

system	cavity radius (Å)	$r_{C\cdots X}$ (Å) (X = Se, S, O)	dipole moment, μ (Debye)	atomic charge (a.u.)	ionization potential (eV)
selenourea, SeU	4.17	1.833	8.18	Se, −0.466; C, 0.113; N, −0.497	5.11
thiourea, SU	4.01	1.702	8.17	S, −0.537; C, 0.236; N, −0.529	6.12
urea, U	3.68	1.224	5.49	O, −0.687; C, 0.669; N, −0.635	7.32

equilibrium process (Scheme 1) is determined by the following equation:[22]

$$\frac{A_0}{A} = 1 + K^{-1}[\mathrm{SeU}]^{-1} \tag{9}$$

where A and A_0 are the absorbance at 410 nm at any given concentration of SeU (6×10^{-6}−1×10^{-3} M) and the saturation absorbance of SeU (1×10^{-3} M) at pH 7, respectively. The plot of $(A_0/A) - 1$ against $[\mathrm{SeU}]^{-1}$ gave a straight line. From the reciprocal of slope, the equilibrium constant (K) is evaluated to be 7.9×10^4 M^{-1}. The equilibrium constant for the formation of a dimer radical cation on reaction with •OH radicals remained almost the same in the pH range of 1−10.

To understand the decay mechanism, the effect of the ionic strength (μ) on the decay rate is studied through the addition of added electrolyte ($NaClO_4$).[38] The following equation is applied to understand the nature of the charge on the reaction partners:[38]

$$\log \frac{k}{k_0} = 1.02 z_1 z_2 \left(\frac{\sqrt{\mu}}{1 + \sqrt{\mu}} \right) \tag{10}$$

k and k_0 are the observed second-order rate constants ($2k/\epsilon$l) in the presence and absence of added $NaClO_4$ (0.02−0.5 M), respectively. The decay rate was observed to increase linearly as the ionic strength increased (see Figure 4d). The slope of the plot (Figure 4d) is positive, which suggests that the electric charges z_1 and z_2 of the reaction partners are of the same sign and that the reaction partners are charged species and, thus, support the reaction mechanism as shown in Scheme 1.

The azide radical is reported to be unreactive toward thiourea[22] but oxidizes SeU to form a transient that absorbs at a wavelength of 410 nm. This indicates that the one-electron oxidation potential of SeU is less than that of thiourea. Pulse radiolysis studies of aqueous solution of urea failed to show any transient absorption in 300−600 nm, even in highly acidic solution (pH 1 and [urea] = 10 mM). This shows that the oxidation of urea is not possible under these experimental conditions. The standard redox couples failed to establish an equilibrium with SeU, and, therefore, the one-electron oxidation potential could not be determined using the pulse radiolysis technique. The cyclic voltammetry studies were performed to evaluate the oxidation potential of SeU and compare it with that of other lighter analogues, such as thiourea and urea. The cyclic voltammograms of selenourea and thiourea showed the oxidation peaks at a potential value of 0.5 and 1.2 V vs SCE, respectively. The cyclic voltammograms of urea have not shown any oxidation peaks between −0.25 V and 1.2 V. Cyclic voltammograms are irreversible in nature, showing that the oxidized species is not stable and is converted to another species.

Theoretical Studies. The conformation of selenourea that has C_{2v} symmetry was determined to be the most-stable structure on full geometry optimization at the BHHLYP/6-31+G(d,p) level. The gas-phase C−Se and C−N bond distances were calculated to be 1.807 and 1.341 Å, respectively, where as the bond angle (∠NCN) was estimated as 115.6°. These bond lengths were modified to 1.833 and 1.331 Å and the angle was enlarged by only 1.0° when the same calculation was repeated including the solvent effect. The solvent effect was included following Onsager's reaction field model with a cavity radius of 3.61 Å. The Mulliken atomic charges over the Se, C, and N atoms were calculated to be −0.466, 0.113, and −0.497 a.u., with the dipole moment of the system being 8.18 D. Table 2 displays a comparison of various calculated properties of selenourea and its lighter analogues. The dipole moment of the system decreased from selenourea to urea, whereas the ionization potential increased from selenourea to urea. The charge on the Se atom was the least negative, compared to that on the S or O atom in the respective systems, because of its less-electronegative nature. The calculated result in regard to the high ionization potential value (7.32 eV) of urea explains the difficulty of its oxidation in comparison to thio or selenourea, as it was also observed in the case of cyclic voltammetry experiments in solution. When the single-electron oxidation of selenourea is performed via ionization or using specific one-electron oxidants in solution, an electron is removed from selenourea and its radical cation is formed. The fully optimized geometry of the selenourea radical cation was also determined to have C_{2v} symmetry at the BHHLYP/6-31+G(d,p) level of theory. The calculated gas-phase C−Se and C−N bond lengths were 1.872 and 1.315 Å, respectively, with an ∠NCN bond angle of 120.6°. The structure of the selenourea radical cation was modified to a minor extent by the inclusion of the solvent effect (cavity radius of 2.97 Å). The C−Se bond length was stretched by 0.043 Å, the C−N bond was shortened by 0.009 Å, and the ∠NCN bond angle was enlarged by only 1.5°. The Mulliken atomic charges over the Se, C, and N atoms were 0.129, 0.216, and −0.453 a.u., respectively, and the dipole moment of the system was calculated to be 9.03 D. The calculated atomic charges for neutral and singly charged selenourea suggest that, when selenourea is oxidized, the electron density is reduced, mainly from the Se site. This is further confirmed by the calculated atomic spin population values in the radical cation of selenourea. The atomic spin populations ($\alpha-\beta$) over the Se and C centers were calculated to be 0.961 and 0.001, respectively, which suggests that the spin population is almost fully localized over the Se center in the radical cation of selenourea. Thus, when the radical cation of selenourea reacts with its unoxidized counterpart, it is expected to react through the Se site and form a dimer radical cation of selenourea. Table 3 displays a comparison of various calculated properties of the selenourea radical cation and its lighter analogues. When single-electron oxidation occurs, the C−X (X = Se, S, O) bond length shortens and the atomic charges mainly change over X. However, the dipole moment shows some anomaly: it increases to a minor extent in the case of selenourea but decreases significantly for thiourea and urea systems.

The gas-phase Se−Se, C−Se, and C−N distances in the most-stable conformer of the selenourea dimer radical cation were calculated to be 2.964, 1.862, and 1.324 Å at the BHHLYP/6-31+G(d,p) level. The bond angles ∠NCN and ∠CSeC were predicted to be 118.8° and 94.7°, respectively. The dihedral angle δ(CSeSeC) was estimated to be −89.6°, and the dipole moment was calculated to be 8.1 D. A depiction of the fully

TABLE 3: Comparison of Different Calculated Properties for Radical Cations of Selenourea, Thiourea, and Urea Including the Solvent Effect

system cation	$r_{C\cdots X}$ (Å) (X = Se, S, O)	atomic charge (a.u.)	dipole moment, μ (Debye)	atomic spin population ($\alpha-\beta$)
selenourea, $SeU^{\bullet+}$	1.915	Se, 0.128; C, 0.216; N, −0.453	9.03	Se, 0.961; C, 0.001
thiourea, $SU^{\bullet+}$	1.752	S, 0.249; C, 0.204; N, −0.485	4.82	S, 0.945; C, 0.031
urea, $U^{\bullet+}$	1.314	O, −0.149; C, 0.691; N, −0.551	3.86	O, 0.921; C, 0.023

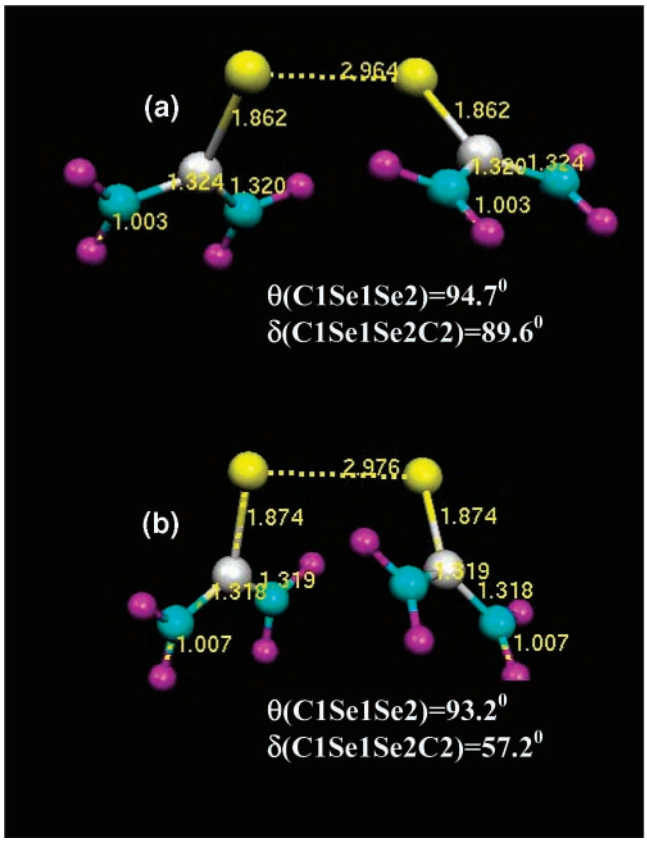

Figure 5. (a) Geometry of the fully optimized most-stable conformer of the selenourea dimer radical cation at the BHHLYP/6-31+G(d,p) level in the gas phase (interatomic distances given in angstroms). The yellow ball refers to the Se atom, ash-gray ball represents the C atom, the blue ball represents the N atom, and the magenta represent sthe H atom. (b) Fully optimized structure of the selenourea dimer radical cation at the BHHLYP/6-31+G(d,p) level with solvent modulation. The solvent effect is included, following Onsager's reaction field model with a cavity radius of 4.17 Å. θ(CSeSe) refers to the angle ∠CSe1Se2, and δ(CSeSeC) refers to the dihedral angle (i.e., the angle between the C1Se1Se2 and Se1Se2C2 planes).

optimized most-stable conformer of the selenourea dimer radical cation in the gas phase is displayed in Figure 5a. The calculation was performed without any symmetry restriction. Symmetry restrictions caused the dimer radical cation system to be less stable, by 14.2 kcal/mol, at the BHHLYP level of theory. The cavity radius of this dimer radical cation species was assumed to be 4.17 Å for solvent effect calculation. The Se···Se distance in solution was calculated to be 2.976 Å. The C−Se and C−N bond distances were modified to 1.874 and 1.318 Å, respectively. The angles ∠CNN and ∠CSeC were affected only to a minor extent, and the respective values were 119.7° and 93.2° with the solvent modulation. However, the solvent effect made a significant change on the dihedral angle, causing the conformation of the dimer radical cation to change significantly in solution, compared to the gas-phase geometry. The new dihedral angle, δ(CSeSeC) = −57.2°, made the dimer radical cation system more compact and the dipole moment of the system increases substantially, to 13.6 D. Because of the shorter dihedral angle, the two dipoles, which correspond to the two monomer groups in the dimer radical cation, cancel, to a lesser extent, in comparison to the gas-phase geometry with a larger dihedral angle. The fully optimized structure of the dimer radical cation of selenourea that has been calculated including the solvent effect is depicted in Figure 5b. The predicted Se···Se distance in solution was observed to be longer by ∼30%, in comparison to the Se−Se single bond length in a crystalline solid of the type X−Se−Se−X.[39] The binding energy (BE) of the dimer radical cation species was calculated to be 21.14 kcal/mol at the BHHLYP/6-31+G(d,p) level, which is ∼20% of the Se−Se single-bond strength. The BE was calculated as the difference between the energy of the dimer radical cation of selenourea and the sum total energy of selenourea and its radical cation. The spin population ($\alpha-\beta$) was distributed equally over two Se atoms, and the value was 0.472 a.u. The bond order between the two Se atoms was 0.41. The calculated weak Se···Se bond strength and bond order being similar to 0.5 for >Se···Se< in the dimer radical cation suggests the possible presence of a *hemi* bond between two Se atoms. Figure 6a depicts the highest doubly occupied molecular orbital (HDOMO) plot of the fully optimized most-stable conformer of the dimer radical cation including the solvent effect. The molecular orbital (MO) clearly indicates the head-on mixing of two valence p-orbitals from two Se atoms and the formation of an *intermolecular two-center three-electron* (2c−3e) σ-bond between two Se atoms (>Se∴Se<) is clearly demonstrated. The lowest singly occupied MO (LSOMO) is displayed in Figure 6b, which shows the antibonding nature of the orbital as the two Se p-orbitals are oriented toward each other with opposite symmetry. This antibonding orbital causes destabilization of the newly formed 2c−3e bond between the two Se atoms and makes the *hemi* bond weak, relative to a two-center, two-electron bond. The calculated results provide a definite indication of the presence of a 2c−3e bond in the dimer radical cation system of selenourea. The same calculations were also performed for the dimer radical cations of the thiourea and urea systems, and various calculated properties are displayed in Table 4. The calculated (BE) for the dimer radical cation of urea is a minimum in the series with the value of 18.39 kcal/mol; however, the changes in BE are small, particularly for selenourea relative to thiourea. However, the two-center, three-electron BE was reported to be much larger for $[H_2O\therefore OH_2]^{\bullet+}$ than that for $[H_2S\therefore SH_2]^{\bullet+}$.[32b] This type of severe effect of substitution on the variation of BE was reported in the literature for $[H_nX\therefore XH_n]^{\bullet+}$ systems with second- and third-row X atoms.[40] It was mentioned that methyl substitution could lead to a significant weakening of the X∴X bond strength when X was a second-row atom. By contrast, the BEs were practically unchanged when the same substitution was made with similar systems between third-row atoms. This contradictory effect was also rationalized through a qualitative analysis that was based on the MO theory of the three-electron bond. Similar arguments should be valid for the present systems. The calculated solvation energy for the selenourea dimer radical cation was 51.13 kcal/mol, which was the highest in the series. The solvation energy was calculated as the difference of the energy of the solvent-modulated optimized structure and the

TABLE 4: Comparison of Different Calculated Solvent-Modulated Properties for Dimer Radical Cations of Selenourea ($(SeU)_2^{\bullet+}$), Thiourea ($(SU)_2^{\bullet+}$), and Urea ($(U)_2^{\bullet+}$)

property	Value		
	$(SeU)_2^{\bullet+}$	$(SU)_2^{\bullet+}$	$(U)_2^{\bullet+}$
$r_{X\cdots X}$ (X = Se, S, O)	2.975 Å	2.808 Å	2.076 Å
dihedral angle, δ(CXXC) (X = Se, S, O)	−57.2°	−76.9°	−139.4°
dipole moment, μ	13.59 Debye	9.77 Debye	4.15 Debye
binding energy, BE	21.14 kcal/mol	20.53 kcal/mol	18.39 kcal/mol
solvation energy	51.13 kcal/mol	46.82 kcal/mol	44.54 kcal/mol
bond order, B_{XX} (X = Se, S, O)	0.41	0.39	0.44
atomic spin population ($\alpha-\beta$)	Se(1), 0.472; Se(2), 0.472	S(1), 0.470; S(2), 0.470	O(1), 0.461; O(2), 0.461

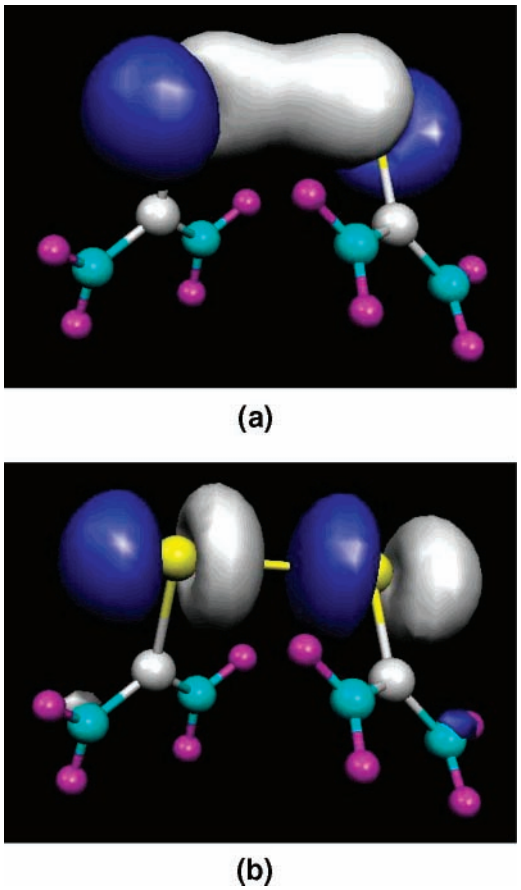

Figure 6. (a) Plot of the highest doubly occupied MO with the maximum contour value of 0.08, showing the presence of a *two-center three-electron* σ-bond between the two Se atoms. The figure shows the head-on mixing of the two valence p-orbitals from two Se atoms in the most-stable conformer of the dimer radical cation of selenourea in solution. (b) Plot of the lowest singly occupied MO in the most-stable geometry with the maximum contour value of 0.08. The two valence p-orbital lobes from two Se atoms are oriented toward each other with opposite symmetry, showing the antibonding sigma nature (σ*) of the orbital.

gas-phase optimized structure at the BHHLYP/6-31+G(d,p) level of theory. The dihedral angle suggests that this is the most-compact structure for the dimer radical cation of selenourea. The calculated dipole moment was the least for the urea system, because of mutual cancellation of the dipole moments by the two parts in the dimer radical cation. In all cases, the atomic spin was mainly populated over Se, S, or O atoms and the spin population was observed to be equally distributed over the two atoms. The calculated bond order in all cases was ~0.4, whereas the expected value was 0.5. For all the optimized structures, a Hessian calculation was performed to examine the reliability of the calculation and determine the frequency of the newly formed *hemi* bond. The Hessian results with no imaginary frequency proved the reliability of the entire calculation. The frequency for the stretching mode of the newly formed >Se∴Se< bond in the selenourea dimer radical cation was predicted to be 215 cm^{-1} at the BHHLYP/6-31+G(d,p) level, based on normal-mode analysis.

Excited-state calculations were performed for both the radical cation and the dimer radical cation of selenourea in the gas phase, as well as in solution, to determine the position of the optical absorption band, λ_{max}. The calculated λ_{max} value, which corresponds to the transition from the highest doubly occupied bonding σ MO (HDOMO) to the lowest singly occupied antibonding σ* MO (LSOMO) in the dimer radical cation of selenourea, was 395 nm, following the CIS procedure. The calculated λ_{max} value was blue-shifted by 15 nm, compared to the solution-phase experimental value of 410 nm. This calculation was performed with the fully optimized geometry of the most-stable conformer of the selenourea dimer radical cation in the gas phase. This $\sigma \rightarrow \sigma^*$ transition was determined to be the lowest electronic transition for this doublet system. When the same excited-state calculation was repeated with the solvent-modulated optimized geometry and orbitals at the BHHLYP/6-31+G(d,p) level of theory, the HDOMO → LSOMO transition was observed to be located at 415 nm, which was red-shifted 5 nm, relative to the reported solution-phase experimental value. This large shift in λ_{max} value is attributed to the large conformational change in the structure of the dimer radical cation of selenourea in solution, compared to that in the gas phase. The similar excited-state calculation, including the solvent effect, suggests that the radical cation of selenourea should absorb at ~240 nm. Thus, it is concluded that the experimental optical absorption band at λ_{max} = 410 nm that is observed in the aqueous solution of selenourea should be due to the *two-center three-electron* bonded dimer radical cation of selenourea.

4. Conclusions

The one-electron oxidation reaction of selenourea in aqueous solution has been studied. Specific one-electron oxidants react with selenourea to form a broad transient optical absorption band at λ_{max} = 410 nm that is attributed to the dimer radical cation. The hydroxyl radical also reacts with selenourea to give a similar transient band at λ_{max} = 410 nm. Based on experimental and ab initio quantum chemical results, the transient band at 410 nm is assigned definitely to the selenourea dimer radical cation. Unlike organic sulfur systems, the dimer radical cation of selenourea reacts with molecular oxygen. The $H^{\bullet}$ atom is also observed to react with selenourea to give the transient optical absorption band of the solute dimer radical cation formed following a H-abstraction reaction. Pulse radiolysis, cyclic voltammetry, and ab inito quantum chemical calculations reveal that selenourea is easily oxidized, in comparison to thiourea. The theoretical result that is based on the ab initio quantum chemical method illustrates the presence of an *intermolecular two-center three-electron* (2c−3e) bond between two Se atoms

in the dimer radical cation of selenourea. Visualization of the highest doubly occupied molecular orbital in the fully optimized stationary geometry of the selenourea dimer radical cation suggests that the Se valence p-orbitals are mixed head-on, resulting in a *hemi* bond of σ nature. The solvent effect shows a red shift in the absorption maxima of the dimer radical cation of selenourea. There is excellent agreement between the experimental and theoretical results, in regard to optical absorption maxima.

Acknowledgment. The Computer Division of Bhabha Atomic Research Centre is gratefully acknowledged for providing the computational facility. We are thankful to Dr. T. Mukherjee for his support.

References and Notes

(1) von Sonntag, C. *The Chemical Basis of Radiation Biology*; Taylor and Francis: London, 1987.

(2) Wardman, P. In *Glutathione Conjugation*; Sies, H., Ketterer, B., Eds.; Academic Press: New York, 1988; p 43.

(3) Wardman, P. In *Sulfur-Centered Reactive Intermediates in Chemistry and Biology*; Chatgiliaoglu, C., Asmus, K.-D., Eds.; NATO ASI Series, A: Life Sciences; Plenum Press: New York, 1990; Vol 197, p 415.

(4) Badiello, R. In *The Chemistry of Organic Selenium and Tellurium Compounds*; Patai, S., Rappoport, Z., Eds.; Wiley: New York, 1986; Vol. 1, p 287.

(5) Mugesh, G.; Singh, H. B. *Chem. Soc. Rev.* **2000**, 347.

(6) Pihl, A.; Sanner, T. In *Radiation Protection and Sensitization*; Morson, H. L., Quintiliani, M., Eds.; Taylor and Francis: London, 1970; p 43.

(7) Klayman, D. L.; Gunther, W. H. H. *Organic Selenium Compounds: Their Chemistry and Biology*; Wiley: New York, 1973.

(8) Shamberger, R. J. *Biochemistry of Selenium*; Plenum Press: New York, 1983.

(9) Nicolaou, K. C.; Petasis, N. A. *Selenium in Natural Products Synthesis*; CIS: Philadelphia, 1984.

(10) Dianez, M. J.; Estrada, M. D.; Lopez-Castro, A. *Carbohydr. Res.* **1993**, *242*, 265.

(11) Asmus, K.-D.; Bonifačič, M. In *Sulfur-Centered Reactive Intermediates as Studied by Radiation Chemical and Complementary Techniques: S-Centered Radicals*; Alfassi, Z. B., Ed.; Wiley: New York, 1999; p 142.

(12) Glass, R. S. *Sulfur Radical Cations: Topics in Current Chemistry*; Springer−Verlag: Berlin, 1999; Vol. 205, p 1.

(13) Asmus, K.-D. In *Sulfur-Centered Reactive Intermediates in Chemistry and Biology*; Chatgiliaoglu, C., Asmus, K.-D., Eds.; NATO ASI Series, A: Life Sciences; Plenum Press: New York, 1990; Vol 197, p 155.

(14) Gawandi, V. B.; Mohan, H.; Mittal, J. P. *J. Phys. Chem. A* **2000**, *104*, 11977.

(15) Maity, D. K.; Mohan, H.; Mittal, J. P. *J. Chem. Soc., Faraday Trans.* **1994**, *90*, 703.

(16) Bobrowski, K.; Schoneich, C.; Holcman, J.; Asmus, K.-D. *J. Chem. Soc., Perkin Trans., 2* **1991**, 975.

(17) Engman, L.; Lind, J.; Merenyi, G. *J. Phys. Chem.* **1994**, *98*, 3174.

(18) Mohan, H.; Mittal, J. P. *J. Phys. Chem. A* **2002**, *106*, 6574.

(19) Korzeniowska-Sobczuk, A.; Hug, G. L.; Carmichael, I.; Bobrowski, K. *J. Phys. Chem. A* **2002**, *106*, 9251.

(20) Ioele, M.; Steennken, S.; Baciocchi, E. *J. Phys. Chem. A* **1997**, *101*, 2979.

(21) Kishore, K.; Dey, G. R.; Moorthy, P. N. *J. Phys. Chem.* **1995**, *99*, 13476.

(22) Wang, W.; Schuchmann, M. N.; Knolle, H. P.; von Sonntag, W. J.; von Sonntag, C. *J. Am. Chem. Soc.* **1999**, *121*, 238.

(23) Stadman, T. C. *Science* **1974**, *183*, 915.

(24) Burk, R. F.; Hill, K. E. *Annu. Rev. Nutr.* **1993**, *13*, 65.

(25) Badiello, R.; Fielden, E. M. *Int. J. Radiat. Biol.* **1970**, *17*, 1.

(26) Mishra, B.; Priyadarsini, K. I.; Sudheer Kumar, M.; Unikrishnan, M. K.; Mohan, H. *Bioorg. Med. Chem.* **2003**, *11*, 2677.

(27) (a) Guha, S. N.; Moorthy, P. N.; Kishore, K.; Rao, K. N. *Proc.—Indian Acad. Sci., Chem. Sci.* **1987**, *99*, 261. (b) Priyadarsini, K. I.; Naik, D. B.; Moorthy, P. N.; Mittal, J. P. *Proceedings of the 7th Tihany Symposium on Radiation Chemistry*; Hungarian Chemical Society: Budapest, Hungary, 1991; p 105.

(28) Fielden, E. M. In *The Study of Fast Processes and Transient Species by Electron Pulse Radiolysis*; Baxendale, J. H., Busi, F., Eds.; D. Reidel: Boston, 1984; p 59.

(29) Panajakar, M. S.; Moorthy, P. N.; Shirke, N. D. BARC Report No. 1410, Bhabha Atomic Research Centre, Mumbai, India, 1988.

(30) Spinks, J. W. T.; Woods, R. J. *An Introduction to Radiation Chemistry*; Wiley: New York, 1990; p 243.

(31) Neta, P.; Huie, R. E.; Ross, A. B. *J. Phys. Chem. Ref. Data* **1988**, *17*, 1027.

(32) (a) Maity, D. K. *J. Am. Chem. Soc.* **2002**, *124*, 8321. (b) Maity, D. K. *J. Phys. Chem. A* **2002**, *106*, 5716. (c) Braïda, B.; Hiberty, P. C.; Savin, A. *J. Phys. Chem. A* **1998**, *102*, 7872.

(33) Braïda, B.; Lauvergnat, D.; Hiberty, P. C. *J. Chem. Phys.* **2001**, *115*, 90.

(34) Schmidt, M. W.; Baldridge, K. K.; Boatz, J. A.; Elbert, S. T.; Gordon, M. S.; Jensen, J. H.; Koseki, S.; Matsunaga, N.; Nguyen, K. A.; Su, S. J.; Windus, T. L.; Dupuis, M.; Montgomery, J. A. *J. Comput. Chem.* **1993**, *14*, 1347.

(35) Stefan, P.; Hans, P. L. *Chimica* **2000**, *54*, 766.

(36) Buxton, G. V.; Greenstock, C. L.; Helman, W. P.; Ross, A. B. *J. Phys. Chem. Ref. Data* **1988**, *17*, 513.

(37) Solar, S.; Solar, W.; Getoff, N.; Holcman, J.; Sehested, K. *J. Chem. Soc., Faraday Trans. 1* **1982**, *78*, 2467.

(38) Lin, S. H.; Li, K. P.; Eyring, H. In *Physical Chemistry. An Advanced Treatise*; Eyring, H., Ed.; Academic Press: New York, 1975; pp 1−58.

(39) Kerr, J. A.; Stocker, D. W. In *CRC Chemistry and Physics Handbook: Strength of Chemical Bonds*; Lide, D. R., Ed.; CRC Press: Boca Raton, FL, 1999; p 9-51.

(40) Braïda, B.; Hazebroucq, S.; Hiberty, P. C. *J. Am. Chem. Soc.* **2002**, *124*, 2371.